The contribution of insects to global forest deadwood decomposition

Sebastian Seibold*, Werner Rammer, Torsten Hothorn, Rupert Seidl, Michael D. Ulyshen, Janina Lorz, Marc W. Cadotte, David B. Lindenmayer, Yagya P. Adhikari, Roxana Aragón, Soyeon Bae, Petr Baldrian, Hassan Barimani Varandi, Jos Barlow, Claus Bässler, Jacques Beauchêne, Erika Berenguer, Rodrigo S. Bergamin, Tone Birkemoe, Gergely Boros, Roland Brandl, Hervé Brustel, Philip J. Burton, Yvonne T. Cakpo-Tossou, Jorge Castro, Eugénie Cateau, Tyler P. Cobb, Nina Farwig, Romina D. Fernández, Jennifer Firn, Kee Seng Gan, Grizelle González, Martin M. Gossner, Jan C. Habel, Christian Hébert, Christoph Heibl, Osmo Heikkala, Andreas Hemp, Claudia Hemp, Joakim Hjältén, Stefan Hotes, Jari Kouki, Thibault Lachat, Jie Liu, Yu Liu, Ya-Huang Luo, Damasa M. Macandog, Pablo E. Martina, Sharif A. Mukul, Baatarbileg Nachin, Kurtis Nisbet, John O'Halloran, Anne Oxbrough, Jeev Nath Pandey, Tomáš Pavlíček, Stephen M. Pawson, Jacques S. Rakotondranary, Jean-Baptiste Ramanamanjato, Liana Rossi, Jürgen Schmidl, Mark Schulze, Stephen Seaton, Marisa J. Stone, Nigel E. Stork, Byambagerel Suran, Anne Sverdrup-Thygeson, Simon Thorn, Ganesh Thyagarajan, Timothy J. Wardlaw, Wolfgang W. Weisser, Sungsoo Yoon, Naili Zhang, Jörg Müller

*corresponding author: sebastian.seibold@tum.de

Affiliations: see attachment

Summary

The amount of carbon stored in deadwood is equivalent to about 8% of global forest carbon stocks[1]. Deadwood decomposition is largely governed by climate[2–5] with decomposer groups, such as microbes and insects, contributing to variations in decomposition rates[2,6,7]. At the global scale, the contribution of insects to deadwood decomposition and carbon release remains poorly understood[7]. Here we present a field experiment of wood decomposition across 55 forest sites on six continents. We find that deadwood decomposition rates increase with temperature, with the strongest temperature effect at high precipitation levels. Precipitation affects decomposition rates negatively at low temperature and positively at high temperatures. As net effect, including direct consumption and indirect effects via interactions with microbes, insects accelerate decomposition in tropical forests (3.9% median mass loss per year). In temperate and boreal forests we find weak positive and negative effects with a median mass loss of 0.9% and -0.1% per year, respectively. Furthermore, we apply the experimentally derived decomposition function to a global map of deadwood carbon synthesised from empirical and remote sensing data. This allows for a first estimate of 10.9 ± 3.2 Pg yr^{-1} of carbon released from deadwood globally, with 93% originating from tropical forests. Globally, the net effect of insects accounts for a carbon flux of 3.2 ± 0.9 Pg yr^{-1} or 29% of the total carbon released from deadwood, which highlights the functional importance of insects for deadwood decomposition and the global carbon cycle.

Main

The world's forests are an important carbon sink[1], but global climate change is affecting carbon sequestration and release by altering tree growth[8,9], mortality[10,11] and decomposition[12,13]. Hence, a comprehensive understanding of the forest carbon cycle and its climate sensitivity is critical for improving global climate change projections. While past research has focused strongly on sequestration[14,15], carbon release, including the decomposition of deadwood, remain poorly understood[7,16]. Deadwood currently stores 73 ± 6 Pg (Petagram, 10^{15} g) of carbon globally, which is about 8% of the global forest carbon stock[1] and 8.5% of atmospheric carbon[17]. Deadwood decomposition is largely governed by climate[2–5], with the activity of different decomposer groups contributing to the considerable variation in decomposition rates[2,6,7]. Recently, the role of fungi in forest carbon cycling has received much attention[2,6] and they are believed to be the principal decomposers of deadwood[5–7]. While local and regional-scale studies indicate that insects can also make a considerable contribution to wood decomposition[7], global assessments quantifying the role of microbes and insects are lacking. Given the sensitivity of insects to climate change[19,20] and the observed declines in insect biodiversity[21–23], a better understanding of the interactions between insect decomposers and climate is needed to more robustly project carbon flux from deadwood and the role of deadwood in the global forest carbon sink[11,16,24].

Here, we quantified the role of deadwood-decomposing insects relative to climate by conducting standardised field experiments of wood decomposition across 55 sites on six continents (Fig. 1a). Our sites were selected to capture the gradient of temperature and precipitation conditions under which forests occur globally. Insects and other animals (hereafter collectively termed insects for brevity) had unrestricted access to wood placed on the forest floor in the *uncaged* treatment in our experiment, while they were excluded from wood in the *closed cage* treatment using mesh cages (Extended Data Fig. 1). Our estimate of the effect of insects on wood decomposition was quantified as the difference between decomposition rates in the *uncaged* and *closed cage* treatments. This measure can be

considered the “net effect of insects”, consisting of direct consumption of wood by insects and indirect effects via interactions with microbes. The latter include, for example, competition for resources, grazing on fungal mycelia, creation of entry ports or vectoring, and can thus either increase[25] or decrease wood decomposition[26,27]. Consequently, direct consumption by insects could be higher than our net estimate where insect-microbe interactions decrease decomposition rates. To explore effects of caging on microclimatic conditions and decomposition rates, we implemented a third treatment (*open cage*) using cages with holes, allowing insects access to wood samples under similar microclimatic conditions to those in the *closed cage* treatment (Supplementary Information section 1). We assessed wood decomposition as mass loss over a period of up to three years for wood samples with bark (~3 cm in diameter, 50 cm in length) of locally dominant native tree species (142 tree species in total) as well as for standardized wooden dowels without bark. In total, we recorded wood mass loss for 4437 individual samples. We used a Gaussian generalized linear mixed log-link model with site-specific random effects to quantify the influence of insects (*uncaged* vs. *closed cage*), site-level temperature and precipitation as well as type of wood (angiosperm vs. gymnosperm) on the annual rates of wood mass loss. Although some influence of caging on microclimate cannot be ruled out, we focused on the comparison between *uncaged* and *closed cage* treatments, because analyses across treatments indicated that this comparison provides the most robust estimate for the net effect of insects on wood decomposition (Supplementary Information section 1; Extended Data Table 1; Extended Data Fig. 2).

To provide a first estimate of the global carbon flux from deadwood decomposition (henceforth referred to as deadwood carbon release) and to quantify the functional importance of insects for global deadwood carbon, we applied the model derived from our decomposition experiment to a novel global deadwood carbon map (Fig. 1a), which we synthesized from empirical and remote-sensing data. As the global modelling of deadwood remains challenging, we conducted in-depth analyses of uncertainty, evaluating the decomposition function derived from our experiment against independent empirical data[28] and quantifying the relative

contribution of different sources of uncertainty in a sensitivity analysis (Supplementary Information section 2 and Extended Data Table 2). The sensitivity analysis also highlights how further research can improve the modelling of global carbon fluxes from deadwood.

Climate and insect effects

In our global experiment, wood decomposition rate was highest in the tropics/subtropics (henceforth called tropics; median = 28.2% mass loss per year), and was considerably lower in the temperate (median = 6.3%) and boreal/hemiboreal (henceforth called boreal; median = 3.3%; Fig. 1b) biomes. Wood decomposition rates were highly climate-sensitive, driven by the complex interplay between temperature and precipitation (Table 1). Decomposition rates increased with increasing temperature across the full gradient of precipitation, but the effects of temperature were strongest at high levels of precipitation (Fig. 2a; Extended Data Fig. 3a). Precipitation affected decomposition rates negatively at low temperatures but positively at high temperatures. The observed positive global relationship between wood decomposition and temperature was similar to patterns observed at local to continental scales[2,4], as well as for the decomposition of non-woody litter[12,29], and is consistent with general theory predicting an increase in metabolic rates and enzymatic activity with temperature[30]. Moreover, the length of the vegetation period usually increases with temperature which may further increase annual decomposition rates. Weaker positive effects of temperature on wood decomposition under low levels of precipitation may be the result of low wood moisture levels, limiting microbial activity[31,32] and selecting for drought-tolerant fungal species which have a reduced ability to decompose wood[6]. Given that temperature is predicted to increase globally[33], our results indicate that wood decomposition rates are likely to increase in the future. The strength of this increase will be modulated by current and future levels of precipitation and the emerging water balance of a site[34]. Decomposition rates were higher for angiosperms than for gymnosperms (Table 1), which is consistent with results from a global meta-analysis and can be explained by differences in wood traits[35]. Results for standardized wooden dowels were similar to those for wood of native tree species (Extended Data Table 1).

Insect access to deadwood affected decomposition, but this effect was contingent on climatic conditions (Table 1). The net effect of insects on decomposition was particularly high in the tropics (median = 3.9% mass loss per year, Fig. 1b). In contrast, effects were low in the temperate biome and even negative in the boreal biome (median of 0.9% and -0.1%, respectively; Fig. 1b). The net effect of insects generally increased with temperature, with effect size strongly mediated by precipitation (Table 1). At low levels of precipitation, temperature had only a minor influence on the net effect of insects. In contrast, at high levels of precipitation, temperature was a strong driver of the net effect of insects on decomposition (Fig. 2b; Extended Data Fig. 3b). At high temperatures, increasing precipitation increased the net effect of insects, while at low temperatures, increasing precipitation resulted in a negative net effect of insects. Thus, decomposition rates were higher when insects were excluded at low temperatures and high precipitation. Complex relationships between insects and climate are driving several mechanisms determining the net effect of insects on wood decomposition. First, wood-feeding termites are a key group of decomposers[7,36], but are largely restricted to regions with high temperatures (Fig. 2b). Nevertheless, considerable variation in the net effect of insects also exists among sites where termites are present (Fig. 2b), underlining the importance of factors beyond termite occurrence. Second, temperature affects the metabolic rate of insects, increasing consumption and accelerating larval development directly[19] as well as indirectly via enhanced food quality[37]. Third, insects can be negatively impacted by high wood moisture when precipitation is high and evaporation low, as is the case e.g. in humid boreal forests (Extended Data Fig. 3b), due to low aeration or high pathogen pressure[38]. Conversely, moisture is a limiting factor at high temperatures, restricting the period of high insect activity to the rainy season[39]. Fourth, interactions of insects and microbes can decrease wood decomposition: Insects, for example, can introduce fungal species which do not contribute significantly to wood decomposition themselves, while suppressing other principal wood-decomposing fungi, thus lowering the overall decomposition rate[26]. In cold and humid regions, such biotic interactions might outweigh the effects of direct consumption, and lead to an overall negative net effect of insects on wood decomposition.

Our findings indicate that wood decomposition is driven by the complex interplay of temperature and precipitation with the decomposer community. Climate warming could accelerate wood decomposition by increasing microbial activity and insect-mediated wood decomposition, particularly where moisture is not limiting. However, increased drying as a result of global change also could decrease deadwood decomposition. Our results support that insect biodiversity loss has the potential to affect deadwood decomposition, but that effects may vary regionally. To improve predictions of the functional effects of biodiversity loss, more research is needed on how specific components of decomposer communities (i.e., biomass, species number, functional composition, species interactions) influence deadwood decomposition[7]. Our work suggests that the strongest functional effects of changes in the decomposer community will occur in regions with warm and humid climate, which should be a particular focus of further research.

Global carbon flux estimate

To assess the role of deadwood decomposition in the global carbon cycle, we applied the relationship between decomposition rates and local climate derived from our global experiment (Table 1) to a map of the global carbon currently stored in deadwood (Fig. 1a). Since our experiment focused on small-diameter deadwood over three years, we adjusted decomposition rates to account for slower mass loss of large-diameter deadwood (for details see Methods and Supplementary Information section 2). We evaluated our relationship between decomposition rate and local climate against 157 independent empirical observations from previous deadwood surveys[28], spanning the full range of deadwood diameters > 7 cm, time since tree death and climatic conditions. We obtained a good match of the results from our model to these independent data (Extended Data Fig. 4), suggesting our approach is robust.

We estimate that 10.9 ± 3.2 Pg carbon might be released from deadwood per year globally. This suggests that deadwood decomposition could be an important flux in the global carbon

cycle . Our estimate corresponds to 15–25% of the annual release of carbon from soils globally (estimated to 50–75 Pg carbon a^{-1} [29]), and is 115% of the current anthropogenic carbon emissions from fossil fuels (9.5 Pg carbon a^{-1} [17]). We note, however, that not all carbon released from deadwood through decomposition is emitted to the atmosphere, as parts are immobilized in the biosphere or in soils[40,41]. Carbon release from deadwood is highest in tropical biomes (10.2 Pg carbon a^{-1}, Fig. 3a, Extended Data Table 3), where large deadwood carbon pools and high decomposition rates coincide (Extended Data Fig. 5). Although deadwood carbon stocks are also considerable in temperate and boreal biomes (amounting to 35% of all carbon stored in deadwood globally), the climatic limitations for wood decomposition as well as differences in decomposer communities (e.g., the absence of termites) render annual carbon fluxes from deadwood much smaller (i.e., 0.44 Pg carbon a^{-1} and 0.28 Pg carbon a^{-1} in boreal and temperate forests, respectively), accounting for less than 7% of the global carbon release from deadwood. Globally, the net effect of insects on wood decomposition may result in a carbon flux of 3.2 ± 0.9 Pg a^{-1}, which represents 29% of the total carbon released from deadwood (Fig. 3a; Extended Data Fig. 5).

Our global estimates are only a first step in a better quantification of the role of deadwood decomposition in the global carbon cycle. Uncertainties related to the underlying data, the statistical models, and other assumptions necessary for upscaling our experimental results were assessed in a global sensitivity analysis. This analysis bounded the uncertainty of global annual carbon release from deadwood and the net effect of insects at approximately ±25% around the mean. Of the various sources of uncertainty that were considered, the underlying data on deadwood carbon stocks contributed most strongly to overall uncertainty (Fig. 3; Extended Data Table 2; Supplementary Information section 2). Our results suggest that global deadwood carbon cycle assessments could be improved by more accurately quantifying deadwood stocks in tropical forests. While the effects of wildfire were included in our deadwood carbon map via the underlying inventory data, we did not explicitly consider deadwood carbon release from fire. We note, however, that a large portion of the carbon

stored in deadwood is not combusted in wildfires[42,43]. Further uncertainty results from our experimental design: It cannot be ruled out that altered microclimatic conditions in cages affected estimates of the net effect of insects derived from the comparison between *closed cage* and *uncaged* treatments. Such a bias would lead to an underestimation of the net insect effect in the tropics and an overestimation in the temperate zone (Supplementary Information section 1). When the global annual net effect of insects on deadwood decomposition was derived from the comparison of *closed cage* and *open cage* treatments, it still amounted to 1.76 Pg carbon. However, this value underestimates the true effect of insects due to reduced insect colonization in the *open cage* treatment (Supplementary Information section 1; Extended Data Fig. 2).

Our experiment highlights that deadwood and wood-decomposing insects play an important role in the global carbon cycle. In contrast to the prevailing paradigm that insects generally accelerate wood decomposition[7], our results indicate that their functional role is more variable, and is contingent on the prevailing climatic conditions. We conclude that ongoing climate warming[33] will likely accelerate decomposition by enhancing the activity of microbes and insects, an effect that will be particularly strong in regions where moisture is not limiting. To robustly project the future of the forest carbon sink[24,44], dynamic global vegetation models need to account for the intricacies of both deadwood creation (e.g., via natural disturbances) and deadwood decomposition.

Main references

1. Pan, Y. *et al.* A large and persistent carbon sink in the world's forests. *Science* **333**, 988–993 (2011).
2. Bradford, M. A. *et al.* Climate fails to predict wood decomposition at regional scales. *Nat. Clim. Chang.* **4**, 625–630 (2014).
3. Chambers, J. Q., Higuchi, N., Schimel, J. P. J., Ferreira, L. V. & Melack, J. M. Decomposition and carbon cycling of dead trees in tropical forests of the central Amazon. *Oecologia* **122**, 380–388 (2000).
4. González, G. *et al.* Decay of aspen (*Populus tremuloides* Michx.) wood in moist and dry boreal, temperate, and tropical forest fragments. *Ambio* **37**, 588–597 (2008).
5. Stokland, J., Siitonen, J. & Jonsson, B. G. *Biodiversity in dead wood*. (Cambridge University Press, 2012).
6. Lustenhouwer, N. *et al.* A trait-based understanding of wood decomposition by fungi. *Proc. Natl. Acad. Sci. U. S. A.* **117**, 1–8 (2020).
7. Ulyshen, M. D. Wood decomposition as influenced by invertebrates. *Biol. Rev. Camb. Philos. Soc.* **91**, 70–85 (2016).
8. Pretzsch, H., Biber, P., Schütze, G., Uhl, E. & Rötzer, T. Forest stand growth dynamics in Central Europe have accelerated since 1870. *Nat. Commun.* **5**, 1–10 (2014).
9. Büntgen, U. *et al.* Limited capacity of tree growth to mitigate the global greenhouse effect under predicted warming. *Nat. Commun.* **10**, 1–6 (2019).
10. Seidl, R. *et al.* Forest disturbances under climate change. *Nat. Clim. Chang.* **7**, 395–402 (2017).
11. Hubau, W. *et al.* Asynchronous carbon sink saturation in African and

Amazonian tropical forests. *Nature* **579**, 80–87 (2020).

12. Portillo-Estrada, M. *et al.* Climatic controls on leaf litter decomposition across European forests and grasslands revealed by reciprocal litter transplantation experiments. *Biogeosciences* **13**, 1621–1633 (2016).

13. Christenson, L. *et al.* Winter climate change influences on soil faunal distribution and abundance: implications for decomposition in the northern forest. *Northeast. Nat.* **24**, B209–B234 (2017).

14. Keenan, T. F. *et al.* Increase in forest water-use efficiency as atmospheric carbon dioxide concentrations rise. *Nature* **499**, 324–327 (2013).

15. Stephenson, N. L. *et al.* Rate of tree carbon accumulation increases continuously with tree size. *Nature* **507**, 90–93 (2014).

16. Martin, A., Dimke, G., Doraisami, M. & Thomas, S. Carbon fractions in the world's dead wood. *Nat. Commun.* 1–9 (2021). doi:10.31223/OSF.IO/SCX3Y

17. Friedlingstein, P. *et al.* Global carbon budget 2019. *Earth Syst. Sci. Data* **11**, 1783–1838 (2019).

18. Ruiz-Peinado, R., Bravo-Oviedo, A., Lopez-Senespleda, E., Montero, G. & Rio, M. Do thinnings influence biomass and soil carbon stocks in Mediterranean maritime pinewoods? *Eur. J. For. Res.* **132**, 253–262 (2013).

19. Marshall, D. J., Pettersen, A. K., Bode, M. & White, C. R. Developmental cost theory predicts thermal environment and vulnerability to global warming. *Nat. Ecol. Evol.* **4**, 406–411 (2020).

20. Buczkowski, G. & Bertelsmeier, C. Invasive termites in a changing climate: A global perspective. *Ecol. Evol.* **7**, 974–985 (2017).

21. Diaz, S., Settele, J. & Brondizio, E. *Summary for policymakers of the global assessment report on biodiversity and ecosystem services of the*

Intergovermental Science-Policy Platform on Biodiversity and Ecosystem Services. (IPBES, 2019).

22. van Klink, R. *et al.* Meta-analysis reveals declines in terrestrial but increases in freshwater insect abundances. *Science* **368**, 417–420 (2020).

23. Seibold, S. *et al.* Arthropod decline in grasslands and forests is associated with landscape-level drivers. *Nature* **574**, 671–674 (2019).

24. Harris, N. L. *et al.* Global maps of twenty-first century forest carbon fluxes. *Nat. Clim. Chang.* (2021). doi:10.1038/s41558-020-00976-6

25. Jacobsen, R. M., Sverdrup-Thygeson, A., Kauserud, H., Mundra, S. & Birkemoe, T. Exclusion of invertebrates influences saprotrophic fungal community and wood decay rate in an experimental field study. *Funct. Ecol.* **32**, 2571–2582 (2018).

26. Skelton, J. *et al.* Fungal symbionts of bark and ambrosia beetles can suppress decomposition of pine sapwood by competing with wood-decay fungi. *Fungal Ecol.* **45**, 100926 (2020).

27. Wu, D., Seibold, S., Ruan, Z., Weng, C. & Yu, M. Island size affects wood decomposition by changing decomposer distribution. *Ecography* (2020). doi:10.1111/ecog.05328

28. Harmon, M. E. *et al.* Release of coarse woody detritus-related carbon: A synthesis across forest biomes. *Carbon Balance Manag.* **15**, 1–21 (2020).

29. Wall, D. H. *et al.* Global decomposition experiment shows soil animal impacts on decomposition are climate-dependent. *Glob. Chang. Biol.* **14**, 2661–2677 (2008).

30. Gillooly, J. F., Brown, J. H., West, G. B., Savage, V. M. & Charnov, E. L. Effects of size and temperature on metabolic rate. *Science* **293**, 2248–2251

(2001).

31. Baldrian, P. *et al.* Responses of the extracellular enzyme activities in hardwood forest to soil temperature and seasonality and the potential effects of climate change. *Soil Biol. Biochem.* **56**, 60–68 (2013).

32. A'Bear, A. D., Jones, T. H., Kandeler, E. & Boddy, L. Interactive effects of temperature and soil moisture on fungal-mediated wood decomposition and extracellular enzyme activity. *Soil Biol. Biochem.* **70**, 151–158 (2014).

33. IPCC. *Climate Change 2014: Synthesis Report. Contribution of Working Groups I, II and III to the Fifth Assessment Report of the Intergovernmental Panel on Climate Change*. (IPCC, 2014).

34. Smyth, C. E., Kurz, W. A., Trofymow, J. A. & CIDET Working Group. Including the effects of water stress on decomposition in the Carbon Budget Model of the Canadian Forest Sector CBM-CFS3. *Ecol. Modell.* **222**, 1080–1091 (2011).

35. Weedon, J. T. *et al.* Global meta-analysis of wood decomposition rates: a role for trait variation among tree species? *Ecol. Lett.* **12**, 45–56 (2009).

36. Griffiths, H. M., Ashton, L. A., Evans, T. A., Parr, C. L. & Eggleton, P. Termites can decompose more than half of deadwood in tropical rainforest. *Curr. Biol.* **29**, R118–R119 (2019).

37. Birkemoe, T., Jacobsen, R. M., Sverdrup-Thygeson, A. & Biedermann, P. H. W. Insect-fungus interactions in dead wood. in *Saproxylic Insects* (ed. Ulyshen, M. D.) 377–427 (Springer, 2018).

38. Harvell, M. C. E. *et al.* Climate warming and disease risks for terrestrial and marine biota. *Science* **296**, 2158–2162 (2002).

39. Berkov, A. Seasonality and stratification: neotropical saproxylic beetles respond to a heat and moisture continuum with conservatism and plasticity. in

Saproxylic Insects (ed. Ulyshen, M. D.) 547–580 (2018).

40. Wang, C., Bond-Lamberty, B. & Gower, S. T. Environmental controls on carbon dioxide flux from black spruce coarse woody debris. *Oecologia* **132**, 374–381 (2002).

41. Peršoh, D. & Borken, W. Impact of woody debris of different tree species on the microbial activity and community of an underlying organic horizon. *Soil Biol. Biochem.* **115**, 516–525 (2017).

42. Campbell, J., Donato, D., Azuma, D. & Law, B. Pyrogenic carbon emission from a large wildfire in Oregon, United States. *J. Geophys. Res. Biogeosciences* **112**, 1–11 (2007).

43. Van Leeuwen, T. T. *et al.* Biomass burning fuel consumption rates: A field measurement database. *Biogeosciences* **11**, 7305–7329 (2014).

44. McDowell, N. G. *et al.* Pervasive shifts in forest dynamics in a changing world. *Science* **368**, eaaz9463 (2020).

Figure legends

Figure 1 | **Decomposition rates and insect effects per biome.** a) Estimated carbon pools in deadwood with diameter >2 cm (Mg C ha^{-1}) with 5 arc minutes spatial resolution and the location of the 55 experimental sites (grey dots). b) Annual mass loss of deadwood of native tree species when all decomposer groups have access (treatment *uncaged*) and c) difference in annual mass loss between *uncaged* and *closed cage* treatments attributed to the net effect of insects. Data show predicted values for both angiosperm and gymnosperm species at 55 and 21 sites, respectively, based on a Gaussian generalized linear mixed log-link model for 2533 logs with site-specific random effects and temperature, precipitation, treatment and host type, as well as their interactions, as fixed effects (Table 1). Boxes represent data within the 25^{th} and 75^{th} percentile, black lines show medians, and whiskers extend to 1.5× the interquartile range. Note that the classification into biomes is shown for illustrative purposes, while the statistical model is based on continuous climate variables.

Figure 2 | **Decomposition rates and net insect effects in climate space.** a) Annual mass loss of deadwood of native tree species, considering all possible groups of decomposers (treatment *uncaged*) and b) annual mass loss attributed to insects (difference in mass loss between treatments *uncaged* and *closed cage*), relative to mean annual temperature and mean annual precipitation. Symbols indicate whether termites occur in the study areas. Points represent predicted values for angiosperm species at 55 sites and gymnosperm species at 21 sites based on a Gaussian generalized linear mixed log-link model for 2533 logs with site-specific random effects and temperature, precipitation, treatment, host division, as well as their interactions, as fixed effects. Note that the lower sample size for gymnosperm species represents their global distribution.

Figure 3 | **Global annual carbon release from deadwood and sensitivity analysis.** a) Annual carbon released (Pg C a^{-1}) from deadwood per biome. Error bars indicate the uncertainty of the biome-specific estimate as determined by the sensitivity analysis. b) Relative

contributions to the overall uncertainty of the global estimate of total carbon release from deadwood decomposition. The color of the bars indicates uncertainty category. See Extended Data Table 2 for a detailed description of each factor and an uncertainty assessment of the net insect effect.

Table 1 | **Drivers of wood decomposition.** Results from a Gaussian generalized linear mixed log-link model for relative annual mass loss of wood of native tree species derived from a global deadwood decomposition experiment. The model is based on data from *closed cage* and *uncaged* treatments, comprising 2533 logs of native tree species from 55 sites. Fixed effects were mean annual temperature and mean annual precipitation sum which were both centered and scaled, host tree type (angiosperm vs. gymnosperm) and treatment, as well as their two- and three-way interactions, with site as random effect. Estimates and standard errors are for temperature and precipitation transformed back to °C and dm a^{-1}. The main effects for each variable are interpretable when the remaining variables are fixed at their reference value (15 °C and 13 dm a^{-1}). A relative effect (i.e., exp(estimate)) of, for instance, 0.989 means that for a temperature increase of 1 °C with all other variables fixed (precipitation at 13 dm a^{-1}, host and treatment), the deadwood dry mass after one year would be 98.9% of the mass without this change in temperature. This represents an additional mass loss of 1.1% induced by a 1 °C increase in temperature. The marginal R^2 of the model was 0.84.

Predictor	**Estimate * 10^3**	**Std.Error * 10^3**	***z*-value**	***p*-value**	**Relative effect and 95% confidence interval**
Temperature (in °C - 15)	-11.009	3.021	-3.644	<0.001	0.989 (0.983 - 0.995)
Precipitation (in dm a^{-1} -13)	-3.135	3.322	-0.944	0.345	0.997 (0.990 - 1.003)
Host: angiosperm	-150.477	22.506	-6.686	<0.001	0.860 (0.823 - 0.899)
Host: gymnosperm	-82.825	24.862	-3.331	0.001	0.921 (0.877 - 0.966)
Treatment: uncaged vs. closed	-29.228	5.694	-5.133	<0.001	0.971 (0.960 - 0.982)
Temperature*precipitation	-0.565	0.401	-1.408	0.159	0.999 (0.999 – 1.000)
Temperature*host	5.016	1.250	4.014	<0.001	1.005 (1.003 - 1.007)
Precipitation*host	-0.434	3.587	-0.121	0.904	1.000 (0.993 - 1.007)
Temperature*treatment	-4.161	0.742	-5.608	<0.001	0.996 (0.994 - 0.997)
Precipitation*treatment	-5.236	0.923	-5.675	<0.001	0.995 (0.993 - 0.997)
Temperature*precipitation*host	0.104	0.327	0.317	0.751	1.000 (0.999 - 1.001)
Temperature*precipitation*treatment	-0.728	0.113	-6.451	<0.001	0.999 (0.999 - 0.999)

Methods

Experimental set-up

We established 55 experimental sites in currently forested areas on six continents and three major biomes, spanning gradients in mean annual temperature from -1.4°C to 27.0°C and mean annual precipitation from 2.90 dm a^{-1} to 33.86 dm a^{-1} (Fig. 1a). Sites were located in mature, closed-canopy stands of the dominant zonal forest type, and were selected so that structural and compositional characteristics were similar to those of natural forests. To quantify the net effect of insects on wood decomposition, we compared decomposition between uncaged wood accessible to all decomposers (treatment *uncaged*) and wood in closed cages excluding insects and other invertebrates (treatment *closed cage*; Extended Data Fig. 1). Cages excluded vertebrate and invertebrate decomposers, but for simplicity, and since insects comprise the functionally most important taxa, we refer to insects throughout the manuscript. To explore microclimatic effects of caging[45], we added a third treatment of wood in cages with large openings (treatment: *open cage*), that allowed colonization by insects, but also provided similar microclimatic conditions as in the *closed cage* treatment (Supplementary Information section 1). Analyses across treatments showed that the most robust assessment of the net effect of insects on wood decomposition originated from the *uncaged* versus *closed cage* treatment, since cages had a significant effect on insect colonization, but not on microclimatic conditions, and thus decomposition rates were reduced in the *open cage* compared to the *uncaged* treatment (Supplementary Information section 1; Extended Data Fig. 2).

Cages measured 40 x 40 x 60 cm and were made of white polyester mesh with 1000 mesh per square inch. The honeycomb-shaped mesh holes had a width of approx. 0.5 mm. Open cages had four rectangular openings measuring 3 x 12 cm at both front sides and four rectangular openings measuring 10 x 15 cm at the bottom, representing in total 6% of the surface area of the cage. Furthermore, open cages had a total of ten 12 cm slits at the top and long sides. Cages were placed on stainless steel mesh (0.5 mm mesh width), which had the

same openings as the bottom side of the cages in the open cage treatment. The top layer of fresh leaf litter was removed before the installation of treatments. The cages and layers of steel mesh were both tightly fixed to the ground using tent pegs, to ensure that all deployed logs had close contact with the soil and to allow water uptake and fungal colonization from the soil. At each site, the three treatments were applied three times, i.e. three installations per treatment per site, resulting in a total of nine installations per site (Extended Data Fig. 1). The nine installations were arranged in a matrix of 3 x 3 with a spacing of 2 m between installations, resulting in a total size of approx. 15 m x 15 m. Treatments were assigned randomly to each of the nine locations within a site. The mean spore size and hyphae width of saprotrophic fungal species (mean spore length and width: 8.9 µm and 5.5 µm[46]; hyphae width: 5-20 µm[47,48]) is by an order of magnitude smaller than the mesh width of our cages. Rhizomorphs, i.e. linear aggregations of several hyphae, can be wider, but during mycelial growth each hypha extends apically rather than the whole rhizomorph[49–51]. Therefore, it is unlikely that the cages hampered fungal colonization. Data loggers recorded air temperature and humidity for the three treatments at nine sites (see Supplementary Information section 1 for details).

Decomposition measurements

Decomposition was measured as mass loss for unprocessed wood of three of the locally most abundant autochthonous tree species at each study site (Supplementary Table S3-1), as well as for standardized machined wooden dowels. Unprocessed wood of local tree species with the bark retained is more likely to be colonized by local insects and fungi than machined wood without bark[45]. The latter was used to compare decomposition based on a standardized substrate replicated across all sites. We cut wood of local tree species (~3 cm in diameter and ~60 cm in length) from either branches or stems of young healthy trees without visible signs of insect or fungal activity. One 5 cm long section was cut from each end of all fresh logs, and the fresh mass of both the cut sections and the resulting 50 cm logs were weighed. The dry mass of all 5 cm sections was measured after drying them at 40°C until no further mass loss was observed. We calculated the dry mass of the respective 50 cm logs as dry mass 50 cm =

(fresh mass 50 cm / fresh mass 5 cm) x dry mass 5 cm. Each installation received three 50 cm long logs of each of the three local tree species and one (*closed cage*) or two (*open cage* and *uncaged*) standardized wooden dowels, giving a total of 96 logs at each site. Standardized dowels (3 cm in diameter, 50 cm in length) were dried machined dowels of *Fagus sylvatica* L. without bark. They were obtained from a single producer in Germany and were then distributed to all sites. Initial dry mass of the dowels was measured directly after drying. All logs and dowels were labeled using numbered plastic tags and assigned randomly to one of the nine installations.

The experiment was established between March 2015 and August 2016 depending on the seasonality of each site. After approximately one, two and three years, one of the three installations of each treatment per site were randomly selected and collected to measure wood decomposition. That is, all logs from one *uncaged*, one *closed cage* and one *open cage* treatment were collected per site at the same time. We chose this approach because the maximum distance between installations was 6 m and thus within-site variation was expected to be rather low. Moreover, we wanted to ensure that the same number of logs could be sampled per treatment and year and failure of cages over time would have resulted in an unbalanced number of logs per treatment. Due to loss of some cages, high decomposition rates at some sites and logistical restrictions, we were not able to maintain the experiment for three years at all sites (Supplementary Table S3-1). Litter and soil attached to the wood was removed carefully upon collection, while fungal fruit bodies were retained. We assessed insect colonization (presence/ absence) for each log based on visible feeding marks, larval tunnels, or exit holes for 3430 (91%) of the analyzed logs. The collected logs were dried at 40°C until mass remained constant and dry mass was measured. At sites where termites were present, logs were burned to account for soil that might have been carried into the wood by these insects[45]. This involved placing one sample at a time onto a steel pan atop a propane burner, and an electrical fan was used to provide aeration and to blow away ash. The residual soil was weighed and its mass subtracted from the dry mass of the wood.

Statistical analyses of the decomposition experiment

All statistical analyses were performed in R version 4.0.4[52]. For each site, we derived information on average climate conditions from WorldClim (v2)[53], specifically BIOMOD variables 1 (mean annual temperature) and 12 (mean annual precipitation sum). We modelled relative wood mass loss of local tree species over time using a Gaussian generalized linear mixed model (function *glmer* in package *lme4*[54]*,* version 1.1.26) with log link. Dry mass of each individual log at time *t* served as the response variable and log-transformed initial dry mass (*t* = 0) was used as an offset term. For each increase of one time unit (one year), the relative reduction is given by exp(*β*). Note that the model contained no intercept due to the constraint $\exp(\beta)^0 = 1$. The rate exp(*β*) was modelled depending on treatment (i.e. *closed cage* versus *uncaged*), and host type (angiosperm versus gymnosperm), as well as mean annual temperature [°C] and mean annual precipitation sum [dm a^{-1}]. Temperature and precipitation were centered and scaled before modelling, but model coefficients were then back-transformed for ease of interpretation. Reference values for temperature and precipitation were 15 °C and 13 dm a^{-1}, respectively. The model included site-specific random time slopes to deal with clustered observations. Based on this model, we computed the fitted annual relative mass loss (in %) for each site considering temperature and precipitation. This was done separately for angiosperm and gymnosperm wood for all sites where respective tree species were present. Note that differences in decomposition between tree species could not be tested but were subsumed in the random slope of the site, since most tree species occurred at only a few sites (Supplementary Table S3-1).

To evaluate potential differences in decomposition rates between the wood of native tree species and standardized wood samples, we estimated the same model for standardized wooden dowels. Further models were fitted to evaluate potential microclimatic effects of the cages on decomposition rates and insect colonization. This included one model for wood decomposition of native tree species for the treatments *closed cage* versus *open cage,* and one model comparing wood decomposition between all three treatment levels (*uncaged,*

closed cage and *open cage*) using a post-hoc test. A binomial generalized linear mixed model was fitted for insect colonization and linear mixed models were fitted for mean daily temperature and mean daily relative humidity. Post-hoc tests were applied to these models for comparisons among the three treatments.

Estimation of global carbon fluxes from deadwood decomposition

To estimate the global carbon flux from deadwood decomposition, we fitted an additive beta regression model (function *gam* with family *betar* in package *mgcv*[55], version 1.8) to site specific predicted relative annual mass loss using temperature and precipitation as predictors, separately for angiosperm and gymnosperm. Based on predicted relative annual mass loss for the *uncaged* treatment, this model was used to predict total deadwood carbon release globally (i.e. attributable to all kinds of decomposers). To quantify the amount of carbon released from deadwood due to the net effect of insects, we applied the beta regression model to predicted relative annual mass loss for the *closed cage* treatment and calculated it as carbon release$_{\text{uncaged}}$ - carbon release$_{\textit{closed cage}}$.

We applied this model to a spatially-explicit global map of carbon stored in deadwood of angiosperms and gymnosperms, which we synthesized from empirical and remote sensing data sets. We used mean annual temperature and mean annual precipitation sum from WorldClim (v2)[53] as predictor data. The GlobBiom (http://globbiomass.org) data set provides high-resolution estimates of forest biomass based on Earth Observation data within the framework of ESA's GlobBiomass project. We used the GlobBiom aboveground biomass layer (i.e., stem, bark, and branch compartments) for the reference year 2010, and aggregated information to the base resolution of WorldClim, i.e., 5 arc minutes (Extended Data Fig. 6a). We extended the aboveground biomass information provided by GlobBiom to total live carbon (including roots) by applying biome-specific root expansion factors[56] and biome-specific biomass to carbon conversion factors between 0.47 and 0.49[16] (Extended Data Fig. 6b). The delineation of forest biomes was taken from FAO[57].

We calculated deadwood carbon stocks at a spatial grain of 5’ by relating deadwood carbon stocks to total live carbon stocks (i.e., deadwood carbon fraction). To quantify regional deadwood carbon fractions, we used data compiled by Pan et al.[1], which are based on forest inventory data and represent the most comprehensive analysis of global forest carbon stocks available to date. We reanalyzed their data set and amended it with data from the FAO Forest Assessment Report[58] where values were missing (Extended Data Table 3). Our estimate of global deadwood carbon stocks therefore reflects local differences in forest productivity, mortality, and land management. The values reported in Pan et al.[1] defined deadwood as “all non-living woody biomass not contained in the litter, either standing, lying on the ground, or in the soil” with a diameter >10 cm. We extended our deadwood carbon pool estimate to include all deadwood >2 cm diameter by applying an expansion factor based on empirical allometric relationships[59]. Our global map of deadwood (Fig. 1a) thus represents the total amount of carbon stored in standing and downed deadwood with a diameter of >2 cm for the reference year 2010.

To differentiate between deadwood of angiosperms and gymnosperms, we used the proportion of broad- and needle-leaved biomass derived from the global land cover product GLCNMO2013[60]. The resolution of GLCNMO2013 is 1/240 degree (i.e., each of our 5’ cells contains 400 land cover pixels), and it provides information on 20 land cover classes. We reclassified these to "Broadleaved", "Needle-leaved", and "Mixed forest", and aggregated to 5’ cells for each of the three forest types. The final proportion of each group was calculated assuming that carbon in mixed forests was equally distributed between angiosperms and gymnosperms (Extended Data Fig. 6c).

The experimental sites were chosen to span the global bioclimatic space inhabited by forests. Nonetheless, gaps remained in very cold and dry climatic conditions for both angiosperm and gymnosperm species as well as in very warm and wet climatic conditions for gymnosperm tree species. We constrained the application of our decomposition models to the climate space covered by the experiment to avoid extrapolation beyond our data. Specifically, we defined

the bioclimatic space for robust predictions via a convex hull around experimental sites in temperature - precipitation space (using a buffer of 3° and 3 dm, respectively). Subsequently, climatic conditions outside that convex hull were mapped to the nearest point within the hull in our modelling (Extended Data Fig. 7).

Our statistical model was derived from deadwood samples with a diameter of ~3 cm, and thus overestimates annual decomposition rates when applied over the full diameter range of deadwood (Supplementary Information section 2). To address this potential bias, we used a conversion factor relating wood mass loss of fine woody debris (FWD, < 10 cm in diameter) to coarse woody debris (CWD, > 10 cm). We based our conversion factor on data from eleven peer-reviewed studies reporting data on both CWD and FWD decomposition, covering all major global biomes (Supplementary Table S2-1). As the relationship of CWD mass loss rate over FWD mass loss rate was robust across different climates, we used its median value (0.53) in our upscaling. An evaluation of the final deadwood decomposition rates used for deriving a first global estimate of the carbon flux from deadwood was performed against independent data from 157 observations compiled by Harmon et al.[28]. This evaluation against independent data indicated good agreement across all major biomes and diameter classes (Extended Data Fig. 4).

Finally, we accounted for the slower carbon release from standing deadwood relative to downed woody debris, particularly in dry regions of the boreal and temperate biome. Based on a wood decomposition data set for standing and downed deadwood across several decay classes for the temperate and boreal biome[61], we estimated decomposition of standing deadwood to be 33-80% slower compared to lying logs. This is consistent with a detailed analysis for temperate forests in Switzerland[62] that found a slowdown of 42%. In the tropics, however, decomposition rates of standing trees have the same or sometimes even higher decomposition rates as downed trees[3,63,64]. We assumed a reduction of decomposition rates by 50% for standing deadwood in temperate and boreal forests, and no reduction in the tropical

biome in our upscaling. Based on large-scale inventories[65–69] we estimated the proportion of standing deadwood on total deadwood as 25% and 30% for the boreal and temperate biome, respectively.

Our global estimate of the carbon fluxes of deadwood decomposition required a number of analytical steps and assumptions, each of which is associated with uncertainties. These can be classified into uncertainties related to deadwood carbon stocks ("Data uncertainties"), uncertainties related to the statistical modelling of deadwood decomposition ("Model uncertainties"), and uncertainties in the upscaling of model results to the global scale ("Scaling uncertainties"). To assess the robustness of our estimate, we performed a global sensitivity analysis[48] where we selected three to four indicators for each of these three categories of uncertainty, and estimated their influence on the overall result. For each of the ten indicators analyzed in total, we selected either a single alternative (e.g., use of the standardized dowels instead of native species) or an upper and lower bound around the default value based on available data or indicator-specific assumptions (Extended Data Table 2). With regard to data uncertainty, we investigated uncertainties associated with the GlobBiom data set used as important data basis here, the deadwood carbon pool estimates[1], and the expansion factors used to derive total biomass from aboveground biomass[56]. Model uncertainties were considered by employing alternative models using the 97.5th and 2.5th percentile of parameter values for fixed effects of the original model, an additional model accounting for potential microclimatic effects of cages (i.e., using the *open cage* instead of the *uncaged* treatment), and a model based on results for the standardized dowels (instead of the native tree species). Lastly, scaling uncertainties were addressed by analyzing alternative expansion factors to include deadwood <10 cm, varying relationships between FWD and CWD decay rate, alternative assumptions regarding the proportion and decay rate of standing deadwood, and the treatment of regions outside of the climate envelope covered by our experiment (see Extended Data Table 2 for details). All factor levels of all indicators were allowed to vary simultaneously, resulting in a total of 4860 estimates for annual deadwood carbon release and

the net effects of insects. The relative influence of each indicator on total uncertainty was derived by means of ANOVA, determining the percent of variance explained by each factor. The contribution at the level of uncertainty categories was derived as the sum of the factors per category. The uncertainty range for the global annual deadwood carbon release estimated from this global sensitivity analysis was ±3.14 Pg, and the net effect of insects varied by ±0.88 Pg carbon. Data uncertainty was identified as the most important factor (~40%), but both model and scaling uncertainty were also highly influential, each contributing 25-30% to the overall variation in the results (Extended Data Table 2).

Methods references

45. Ulyshen, M. D. & Wagner, T. L. Quantifying arthropod contributions to wood decay. *Methods Ecol. Evol.* **4**, 345–352 (2013).

46. Bässler, C., Heilmann-Clausen, J., Karasch, P., Brandl, R. & Halbwachs, H. Ectomycorrhizal fungi have larger fruit bodies than saprotrophic fungi. *Fungal Ecol.* **17**, 205–212 (2015).

47. Ryvarden, L. & Gilbertson, R. L. *The Polyporaceae of Europe*. (Fungiflora, 1994).

48. Eriksson, J. & Ryvarden, L. *The Corticiaceae of North Europe Part 1-8*. (Fungiflora, 1987).

49. Boddy, L., Hynes, J., Bebber, D. P. & Fricker, M. D. Saprotrophic cord systems. dispersal mechanisms in space and time. *Mycoscience* **50**, 9–19 (2009).

50. Moore, D. *Fungal Morphogenesis*. (Cambridge University Press, 1998).

51. Clemencon, H. *Anatomy of the Hymenomycetes*. (Universtity of Lausanne, 1997).

52. R Core Team. R: A language and environment for statistical computing. (2020).

53. Fick, S. E. & Hijmans, R. J. WorldClim 2: new 1-km spatial resolution climate surfaces for global land areas. *Int. J. Climatol.* **37**, 4302–4315 (2017).

54. Bates, D., Maechler, M., Bolker, B. & Walker, S. Fitting linear mixed-effects models using lme4. *J. Stat. Softw.* **67**, 1–48 (2015).

55. Wood, S. N. *Generalized Additive Models: an introduction with R (2nd edition)*. (Chapman and Hall/CRC, 2017).

56. Robinson, D. Implications of a large global root biomass for carbon sink

estimates and for soil carbon dynamics. *Proc. R. Soc. B Biol. Sci.* **274**, 2753–2759 (2007).

57. Food and Agriculture Organization. *Global ecological zones for FAO forest reporting: 2010 Update, Forest Resource Assessment Working Paper*. (Food and Agriculture Organization, 2012).

58. Food and Agriculture Organization. *Global Forest Resources Assessment 2015*. (Food and Agriculture Organization, 2016).

59. Müller-Using, S. & Bartsch, N. Decay dynamic of coarse and fine woody debris of a beech (*Fagus sylvatica* L.) forest in Central Germany. *Eur. J. For. Res.* **128**, 287–296 (2009).

60. Kobayashi, T. *et al.* Production of global land cover data – GLCNMO2013. *J. Geogr. Geol.* **9**, 1 (2017).

61. Harmon, M. E., Woodall, C. W., Fasth, B., Sexton, J. & Yatkov, M. *Differences between standing and downed dead tree wood density reduction factors: A comparison across decay classes and tree species*. *U.S. Department of Agriculture, Forest Service, Northern Research Station, Research Paper NRS-15* (2011).

62. Hararuk, O., Kurz, W. A. & Didion, M. Dynamics of dead wood decay in Swiss forests. *For. Ecosyst.* **7**, (2020).

63. Gora, E. M., Kneale, R. C., Larjavaara, M. & Muller-Landau, H. C. Dead wood necromass in a moist tropical forest: stocks, fluxes, and spatiotemporal variability. *Ecosystems* **22**, 1189–1205 (2019).

64. Hérault, B. *et al.* Modeling decay rates of dead wood in a neotropical forest. *Oecologia* **164**, 243–251 (2010).

65. Thünen-Institut für Waldökosysteme. *Der Wald in Deutschland - Ausgewählte*

Ergebnisse der dritten Bundeswaldinventur. (Bundesministerium für Ernährung und Landwirtschaft, 2014).

66. Puletti, N. *et al.* A dataset of forest volume deadwood estimates for Europe. *Ann. For. Sci.* **76**, 1–8 (2019).

67. Richardson, S. J. *et al.* Deadwood in New Zealand's indigenous forests. *For. Ecol. Manage.* **258**, 2456–2466 (2009).

68. Shorohova, E. & Kapitsa, E. Stand and landscape scale variability in the amount and diversity of coarse woody debris in primeval European boreal forests. *For. Ecol. Manage.* **356**, 273–284 (2015).

69. Szymañski, C., Fontana, G. & Sanguinetti, J. Natural and anthropogenic influences on coarse woody debris stocks in Nothofagus–Araucaria forests of northern Patagonia, Argentina. *Austral Ecol.* **42**, 48–60 (2017).

Data availability

Raw data from the global deadwood experiment, our global map of deadwood carbon and our map of predicted decomposition rates are publicly available from figshare https://figshare.com/s/ffc39ee0724b11bf450c (doi: 10.6084/m9.figshare.14545992).

Code availability

An annotated R code including the data needed to reproduce the statistical analyses, global estimates, and sensitivity analysis is publicly available from figshare https://figshare.com/s/ffc39ee0724b11bf450c (doi: 10.6084/m9.figshare.14545992).

Acknowledgments

We thank the administration of the Bavarian Forest National Park for financing the setup of the experiment and all members of the local teams for their contribution in the field and

laboratory. We especially thank David Blair who operated the site in Victoria, Australia, until his unexpected death in 2019. We thank Bodo von Rentzel, Jörg Ganzhorn, Axel Gruppe, Mark Harmon, Sandra Muller and Sandra Irwin, Makiling Center for Mountain Ecosystems, University of the Philippines Los Banos, the Ministerio del Ambiente de Ecuador, the Instituto Nacional de Biodiversidad de Ecuador and the foundation “Nature and Culture International” for their support. S.S. was supported by the German Academic Exchange Service (DAAD) with funds from the German Federal Ministry of Education and Research and the People Programme of the European Union (Marie Curie Actions; grant number 605728). N.F. was supported by the German Research Foundation (FA925/7-1, FA925/11-1).

Author information

Affiliations

Ecosystem Dynamics and Forest Management Group, Technical University of Munich, Freising, Germany
S. Seibold, R. Seidl & W. Rammer
Berchtesgaden National Park, Berchtesgaden, Germany
S. Seibold & R. Seidl
Epidemiology, Biostatistics, and Prevention Institute, University of Zurich, Zurich, Switzerland
T. Hothorn
Field Station Fabrikschleichach, University of Würzburg, Rauhenebrach, Germany
J. Müller, J. Lorz & S. Thorn
Southern Research Station, USDA Forest Service, Athens, GA, USA
M. D. Ulyshen
Fenner School of Environment and Society, The Australian National University, Canberra, ACT, Australia
D. B. Lindenmayer
Department of Biogeography, University of Bayreuth, Bayreuth, Germany
Y. P. Adhikari
Department of Disturbance Ecology, University of Bayreuth, Bayreuth, Germany
Y. P. Adhikari
Instituto de Ecología Regional, CONICET-Universidad Nacional de Tucumán, Yerba Buena, Tucumán, Argentina

R. Aragón & R. D. Fernández
Department of Animal Ecology and Tropical Biology, University of Würzburg, Würzburg, Germany
S. Bae
Laboratory of Environmental Microbiology, Institute of Microbiology of the Czech Academy of Sciences, Praha, Czech Republic
P. Baldrian
Agricultural and Natural Resources Research Centre of Mazandaran, Sari, Iran
H. Barimani Varandi
Lancaster Environment Centre, Lancaster University, Lancaster, UK
E. Berenguer & J. Barlow
Universidade Federal de Lavras, Lavras, Brazil
J. Barlow
Department of Biodiversity Conservation, Goethe-University Frankfurt, Frankfurt, Germany
C. Bässler
Bavarian Forest National Park, Grafenau, Germany
J. Müller, C. Bässler & C. Heibl
CIRAD, UMR Ecologie des Forêts de Guyane (EcoFoG), AgroParisTech, CNRS, INRA, Universite des Antilles, Universite de Guyane, Kourou, France
J. Beauchêne
Environmental Change Institute, University of Oxford, Oxford, UK
E. Berenguer
Grassland Vegetation Lab, Federal University of Rio Grande do Sul, Brazil
R. S. Bergamin
Faculty of Environmental Sciences and Natural Resource Management, Norwegian University of Life Sciences, Aas, Norway
A. Sverdrup-Thygeson & T. Birkemoe
Institute of Ecology and Botany, Centre for Ecological Research, Vácrátót, Hungary
G. Boros
Department of Zoology and Animal Ecology, Szent István University, Gödöllő, Hungary
G. Boros
Animal Ecology, University of Marburg, Marburg, Germany
R. Brandl
École d'Ingénieurs de Purpan, Université de Toulouse, Toulouse, France
E. Cateau & H. Brustel

Ecosystem Science and Management Program, University of Northern British Columbia, Terrace, B.C., Canada
P. J. Burton
Biological Sciences, University of Toronto Scarborough, Toronto, ON, Canada
M. W. Cadotte
Laboratory of Applied Ecology, University of Abomey-Calavi, Benin
Y. T. Cakpo-Tossou
Department of Ecology, University of Granada, Granada, Spain
J. Castro
Réserves Naturelles de France, Dijon, France
E. Cateau
Royal Alberta Museum, Edmonton, Alberta, Canada
T. P. Cobb
Conservation Ecology, University of Marburg, Marburg, Germany
N. Farwig
Science and Engineering Faculty, Queensland University of Technology, Brisbane, Australia
J. Firn
Centre for the Environment, Institute for Future Environments, Brisbane, Australia
J. Firn
Forest Research Institute Malaysia, Malaysia
K. Gan
International Institute of Tropical Forestry, USDA Forest Service, San Juan, PR, USA
G. González
Swiss Federal Research Institute WSL, Birmensdorf, Switzerland
M. M. Gossner & T. Lachat
Evolutionary Zoology, University of Salzburg, Salzburg, Austria
J. C. Habel
Natural Resources Canada, Canadian Forest Service, Quebec, Canada
C. Hébert
Eurofins Ahma Oy, Oulu, Finland
O. Heikkala
Department of Plant Systematics, University of Bayreuth, Bayreuth, Germany
A. Hemp & C. Hemp
Department of Wildlife, Fish, and Environmental Studies, Swedish University of Agricultural Sciences, Umeå, Sweden
J. Hjältén

Applied Landscape Ecology, Chuo University, Tokyo, Japan
S. Hotes
School of Forest Sciences, University of Eastern Finland, Joensuu, Finland
J. Kouki
School of Agricultural, Forest and Food Sciences, Bern University of Applied Sciences, Zollikofen, Switzerland
T. Lachat
CAS Key Laboratory for Plant Diversity and Biogeography of East Asia, Kunming Institute of Botany, Chinese Academy of Sciences, Kunming, China
J. Liu & Y. Luo
ECNU-Alberta Joint Lab for Biodiversity Study, Tiantong National Station for Forest Ecosystem Research, East China Normal University, Shanghai, China
Y. Liu
Institute of Biological Sciences, University of the Philippines Los Banos, Laguna, Philippines
D. M. Macandog
Department of Thermodynamics, Universidad Nacional del Nordeste, Resistencia, Argentina
P. E. Martina
Tropical Forests and People Research Centre, University of the Sunshine Coast, Maroochydore, QLD, Australia
S. A. Mukul
Forest Ecosystem Monitoring Laboratory, National University of Mongolia, Ulaanbaatar, Mongolia
B. Nachin & B. Suran
School of Environment and Science, Griffith University, Nathan, QLD, Australia
K. Nisbet
School of Biological, Earth and Environmental Sceinces, University College, Cork, Ireland
J. O'Halloran
Edge Hill University, Ormskirk, Lancashire, UK
A. Oxbrough
Institute of Forestry, Tribhuvan University, Pokhara, Nepal
J. Pandey
Institute of Evolution, University of Haifa, Haifa, Israel
T. Pavlíček
Scion (New Zealand Forest Research Institute), Christchurch, New Zealand

S. M. Pawson
School of Forestry, University of Canterbury, Christchurch, New Zealand
S. M. Pawson
Institute of Zoology, University of Hamburg, Hamburg, Germany
J. S. Rakotondranary
Faculté des Sciences, Université d'Antananarivo, Antananarivo, Madagascar
J. S. Rakotondranary
Tropical Biodiversity and Social Enterprise, Fort-Dauphin, Madagascar
J. Ramanamanjato
Departamento de Ecologia, Universidade Estadual Paulista, Rio Claro, SP, Brazil
L. C. Rossi
Ecology group, University Erlangen-Nuremberg, Erlangen, Germany
J. Schmidl
H.J. Andrews Experimental Forest, Blue River, OR, USA
M. Schulze
Environmental and Conservation Sciences, Murdoch University, Melville, WA, Australia
S. Seaton
Environmental Futures Research Institute, Griffith University, Nathan, QLD, Australia.
M. J. Stone & N. E. Stork
Ashoka Trust for Research in Ecology and the Environment, Bangalore, India
G. Thyagarajan
School of Plant Sciences, University of Tasmania, Australia
T. J. Wardlaw
Terrestrial Ecology Research Group, Technical University of Munich, Freising, Germany
W. W. Weisser
EcoBank Team, National Institute of Ecology, Seocheon-gun, Republic of Korea
S. Yoon
College of Forestry, Beijing Forestry University, Beijing, China
N. Zhang

Contributions

S.S., J.M., R.S. perceived the idea of this manuscript. S.S., J.M. and M.U. designed the experiment. S.S., J.L., W.R., M.U., Y.A., R.A., S.B., H.Ba., J.Ba., J.Be., E.B., R.Be., T.B., G.B.,

H.Br., P.Bu., M.C., Y.C., J.C., E.C., T.C., N.F.,R.F., J.F., K.G., G.G., J.H., C.Heb., O.H., A.H., C.H., J.H., S.H., J.K., T.L., D.L., J.L., Y.Li., Y.Lu., D.M., P.M., S.M., B.N., K.N., J.O., A.O., T.P., S.P., J.Rak., J.Ram., L.R., M.Sc., S.Sea., M.St., N.S., B.S., A.S., G.T., T.W., S.Y., N.Z., J.M collected data. S.S., T.H., and W.R. analyzed the data. S.S., J.M., R.S. and W.R. wrote the first manuscript draft with significant inputs from M.U., M.C. and D.L., and finalized the manuscript. All authors commented on the manuscript.

Corresponding author

Correspondence to Sebastian Seibold sebastian.seibold@tum.de

Ethics declarations

Competing interests

The authors declare no competing interests.

Additional Information

Supplementary Information This file contains supplementary information about methods, descriptions of supplementary analyses and a detailed discussion addressing methodological challenges.

Extended Data Table 1 **| Supporting analyses of drivers of wood decomposition.** Results from Gaussian generalized linear mixed log-link models for relative annual mass loss of a) standardized wooden dowels comparing the treatments *uncaged* versus *closed cage* (415 logs from 55 sites) and b) wood of native tree species comparing the treatments *open cage* and *closed cage* 2522 logs from 55 sites). Models include mean annual temperature and mean annual precipitation sum which were both centered and scaled, host tree type (angiosperm vs. gymnosperm; in model b only) and treatment, as well as their two- and three-way interactions, as fixed effects and site as the random effect. Estimates and standard error are for temperature and precipitation transformed back to °C and dm a^{-1}. The main effects of each variable is interpretable when the remaining variables are fixed at their reference value (15°C and 13 dm a^{-1}).

Extended Data Table 2 | **Uncertainty in global carbon fluxes from deadwood decomposition, determined in a global sensitivity analysis.** Important factors per uncertainty category were selected and allowed to vary simultaneously, resulting in a total of 4860 analyzed combinations. The uncertainty of total annual deadwood carbon released and of the net effect of insects was calculated as the standard deviation over all combinations for each factor, with all other factors fixed to their default value. Similarly, the uncertainty per category was calculated over all combinations within a category, with all factors from other categories fixed to the default value. The relative contribution of each factor to overall uncertainty was derived by means of an ANOVA, estimating the percent of variance explained for each factor. The contribution at the level of uncertainty categories is the sum of the respective factors in each category. CI = confidence interval; FWD= fine woody debris; CWD= coarse woody debris; SWD= standing woody debris; DWD= downed woody debris.

Extended Data Table 3 | **Comparison of global carbon stock estimates and results for biomes. a**) Global estimates of total live carbon and carbon in deadwood (>10 cm) from Pan et al.[1] compared with estimates obtained in this study (>2 cm) in Pg. Numbers in brackets indicate the difference in percent. Note that Pan et al.[1] defined biomes at country level while

898 we here define biomes using the FAO Global Ecological Zones. Differences between these
899 biome definitions are especially significant for the temperate biome, as temperate parts of
900 Russia and Canada are included in the boreal biome in Pan et al.[1], while we here divide Russia
901 and Canada into boreal and temperate regions. Furthermore, missing and unrealistic
902 deadwood carbon stocks for a number of areas (specifically Japan, South Korea, China,
903 Australia, and Alaska) in Pan et al.[1] were complemented with data from the FAO Forest
904 Assessment Report[58] in this study, which contributes to higher deadwood carbon estimates
905 relative to Pan et al.[1]. **b**) annual deadwood carbon release and net insect effect per biome (in
906 Pg), and calculated residence time of deadwood carbon (years).

907

Extended Data Figure 1 | **Arrangement of installations per site and treatments.** a) Each site received three installations of three treatments randomly assigned to a 3 x 3 grid. Treatments included b) closed cages to exclude insects, c) open cages providing similar microclimatic conditions as closed cages but giving access to insects and d) uncaged bundles of logs. Cages measured 40 x 40 x 60 cm and were made of white polyester with honeycomb-shaped meshes with a side length of approx. 0.5 mm. Open cages had four rectangular openings measuring 3 x 12 cm at both front sides and four rectangular openings measuring 10 x 15 cm at the bottom representing in total 6% of the surface area of the cage as well as a total of ten 12 cm slits at the top and long sides. All cages were placed on stainless steel mesh (0.5 mm mesh width), which had the same openings as the bottom side of the cages in the open cage treatment. Photographs show the site in the Bavarian Forest National Park, Germany.

Extended Data Figure 2 | **Effects of treatments on wood decomposition and insect colonization.** Coefficients and confidence intervals from post-hoc tests assessing all three pairwise comparisons between the *uncaged, closed cage* and *open cage* treatments for a) annual mass loss (same structure as the model shown in Table 1 based on 3578 logs) and b) insect colonization (binomial model for insect presence and absence based on 3430 logs) of wood of native tree species. 95% confidence intervals not intersecting the zero line (dashed) indicate significant differences. c) Pairwise comparison of fitted annual mass loss (in %) between each of the three treatments in the global deadwood decomposition experiment. Points represent predicted values for angiosperm species at 55 sites and gymnosperm species at 21 sites based on three Gaussian generalized linear mixed log-link models for 3758 logs with site-specific random effects and temperature, precipitation, treatment (*closed cage* versus *uncaged, open cage* versus *uncaged* and *closed cage* versus *open cage*, respectively), host division, as well as their interactions, as fixed effects.

In a) and b), largest differences in both response variables were observed between *uncaged* and *closed cage* treatments. Annual mass loss was higher in *uncaged* than *open cages* and

higher in *open cages* than in *closed cages*, although the latter was not significant. This indicates that the *open cage*, despite its openings for insects, has a clearly reduced decomposition rate compared to the *uncaged* treatment. Insect colonization for the *open cage* differed significantly from both *uncaged* and *closed cage*, but was more similar to *uncaged* than *closed cage*. This indicates that *open cages* were colonized by insects, but not as frequently as the *uncaged* treatment. *Open cages* thus excluded parts of the wood-decomposing insect community, which may explain the rather small difference in annual mass loss between *closed cage* and *open cages*. These results suggest that the comparison of *uncaged* versus *closed caged* provides a more reliable estimate of the net effect of insects on wood decomposition than the comparison of *closed cage* versus *open cage* treatments, which is likely underestimating the net effect of insects. In c), the difference between annual mass loss in *closed cage* and both treatments with insect access (*uncaged* and *open cage*) increased from boreal to tropical, whereas the difference between *uncaged* and *open cage* hardly deviated from the 1:1 line. This indicates that the reported mass loss differences between *closed cage* and *uncaged* treatments, as well as the accelerating effect of temperature and precipitation (Table 1), can be attributed to insects and are not an artefact of potential microclimatic effects of the cages (Supplementary Information section 1).

Extended Data Figure 3 | **Interaction effects of temperature and precipitation on wood decomposition.** Predictions based on the model presented in Table 1 for a) annual mass loss of deadwood of native tree species (2533 logs at 55 sites), considering all possible groups of decomposers (treatment *uncaged*) and b) annual mass loss attributed to insects (difference in mass loss between treatments *uncaged* and *closed cage*), relative to temperature and precipitation. The length of the lines is limited to the gradients in precipitation covered by the sites.

Extended Data Figure 4 | **Model evaluation against independent data**. Comparison of 157 independent observations of annual deadwood decomposition rates measured for larger diameter wood in previous deadwood surveys (red dots, Harmon et al.[28]) with the predictions from our model for the same locations (blue triangles). Lines indicate the relationship between decomposition rate and mean annual temperature from Harmon et al.[28] (red dashed line, $k=0.0184e^{0.0787*temperature}$) and for our model (blue line, $k=0.0171e^{0.0812*temperature}$). Good correspondence of both curves indicates that our models of global carbon release from deadwood provide robust estimates despite being based on experimental deadwood with ~3 cm diameter (for detailed discussion, see Supplementary Information section 1).

Extended Data Figure 5 | **Global deadwood carbon fluxes.** a) Total annual release of deadwood carbon from decomposition including all decomposers and b) annual release of deadwood carbon due to the net effect of insects. Light grey areas indicate values of ±0.1 Mg carbon ha^{-1} a^{-1} and white areas are non-forest systems. c) Latitudinal distribution of global deadwood carbon fluxes per hectare.

Extended Data Figure 6 | **Processing steps for the global deadwood carbon map** a) Aboveground forest biomass (Mg ha^{-1}) aggregated to 5' from the GlobBiom data set. b) Total live carbon (Mg ha^{-1}) by extending a) with root biomass[56] and conversion to carbon. c) Proportion of gymnosperm forests derived from the GLCNMO2013[60] data set. The proportion of angiosperm cover is 1 – gymnosperm cover. White = non-forested area.

Extended Data Figure 7 | **Bioclimatic space for robust predictions.** Climate conditions outside of the range of prediction models for a) angiosperm and b) gymnosperm species in climate space (left) and mapped (right). Left: dark-blue points are outside of the range defined by a convex hull around the experimental sites (black triangles). Right: The colors on the maps indicate the absolute difference between the local climate and the climate used for prediction for temperature (red color channel) and precipitation (blue color channel) with black meaning no difference. White areas indicate that no gymnosperm or angiosperm forest, respectively,

986 occurs here. Experimental sites are indicated by yellow dots. Temperatures outside of the
987 range are mainly located in north-eastern Siberia and northern Canada, whereas offsets in
988 precipitation are stronger for gymnosperms in south-eastern Asia, Indonesia, and in the
989 Amazon region. The land surface area not covered by our experimental data is 23.5% for
990 gymnosperms and 17.7% for angiosperms, representing together 13.2% of the C stored in
991 deadwood. These areas were included in our upscaling by mapping them to the nearest point
992 at the convex hull in climate space.

993

a Deadwood carbon pool

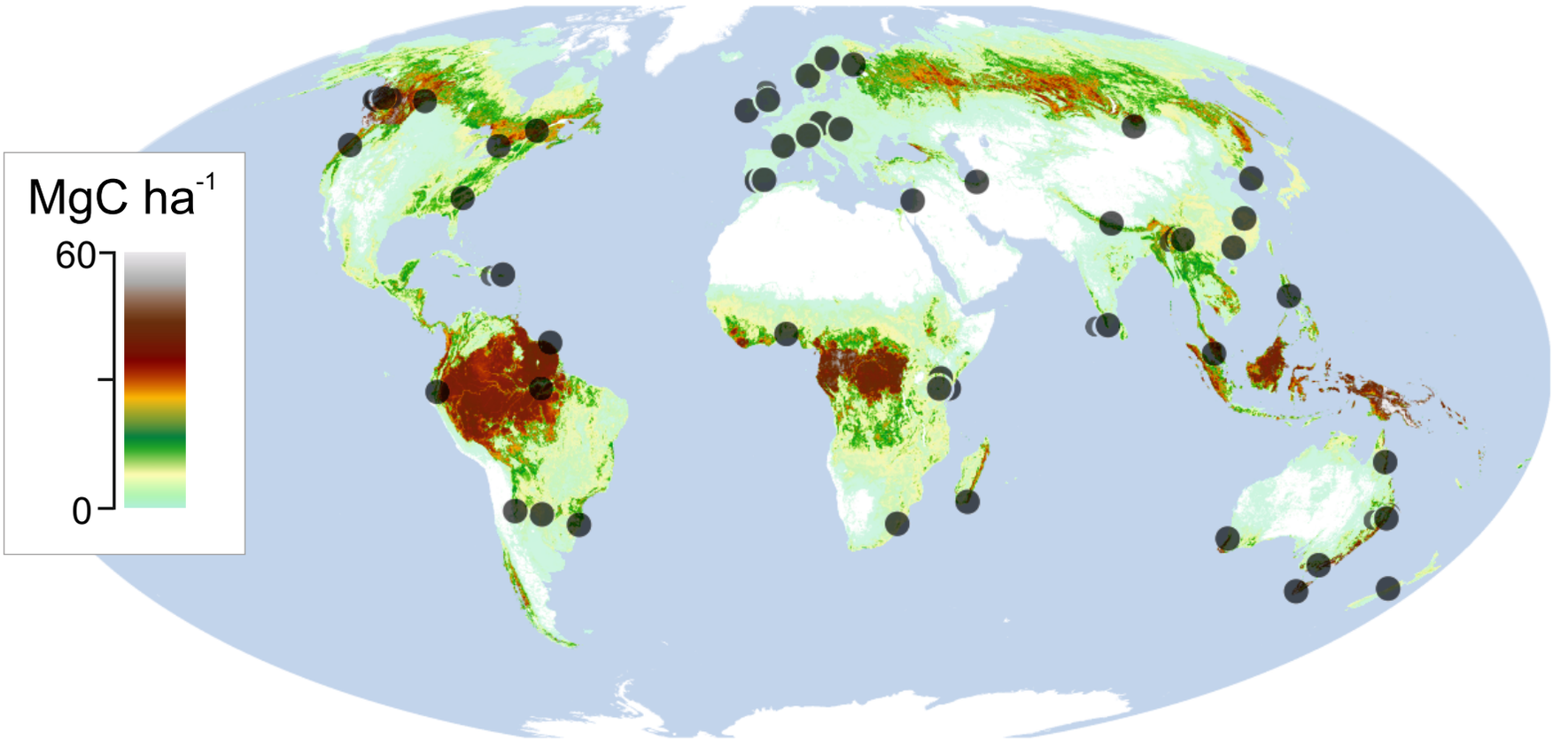

b Annual mass loss

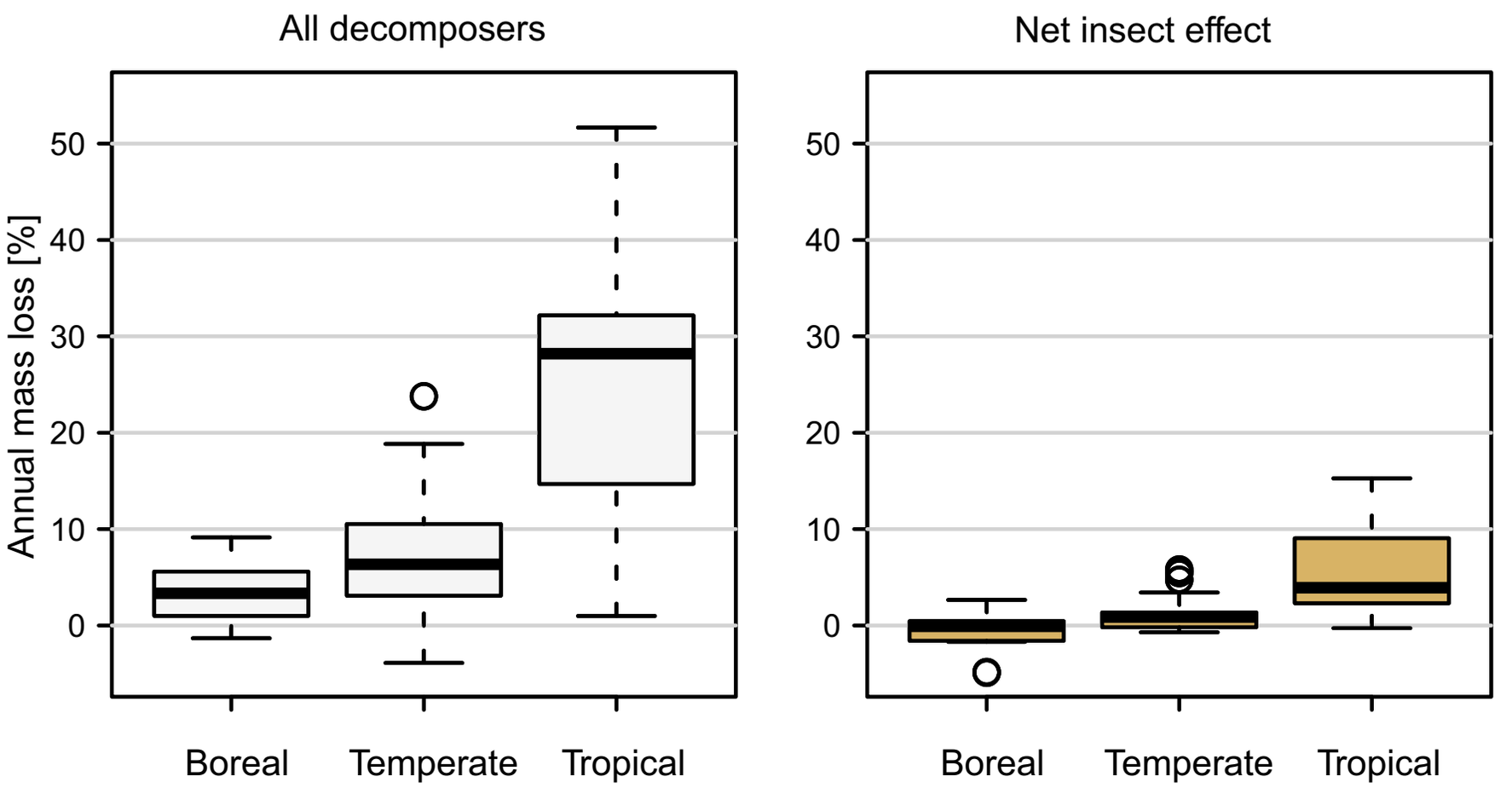

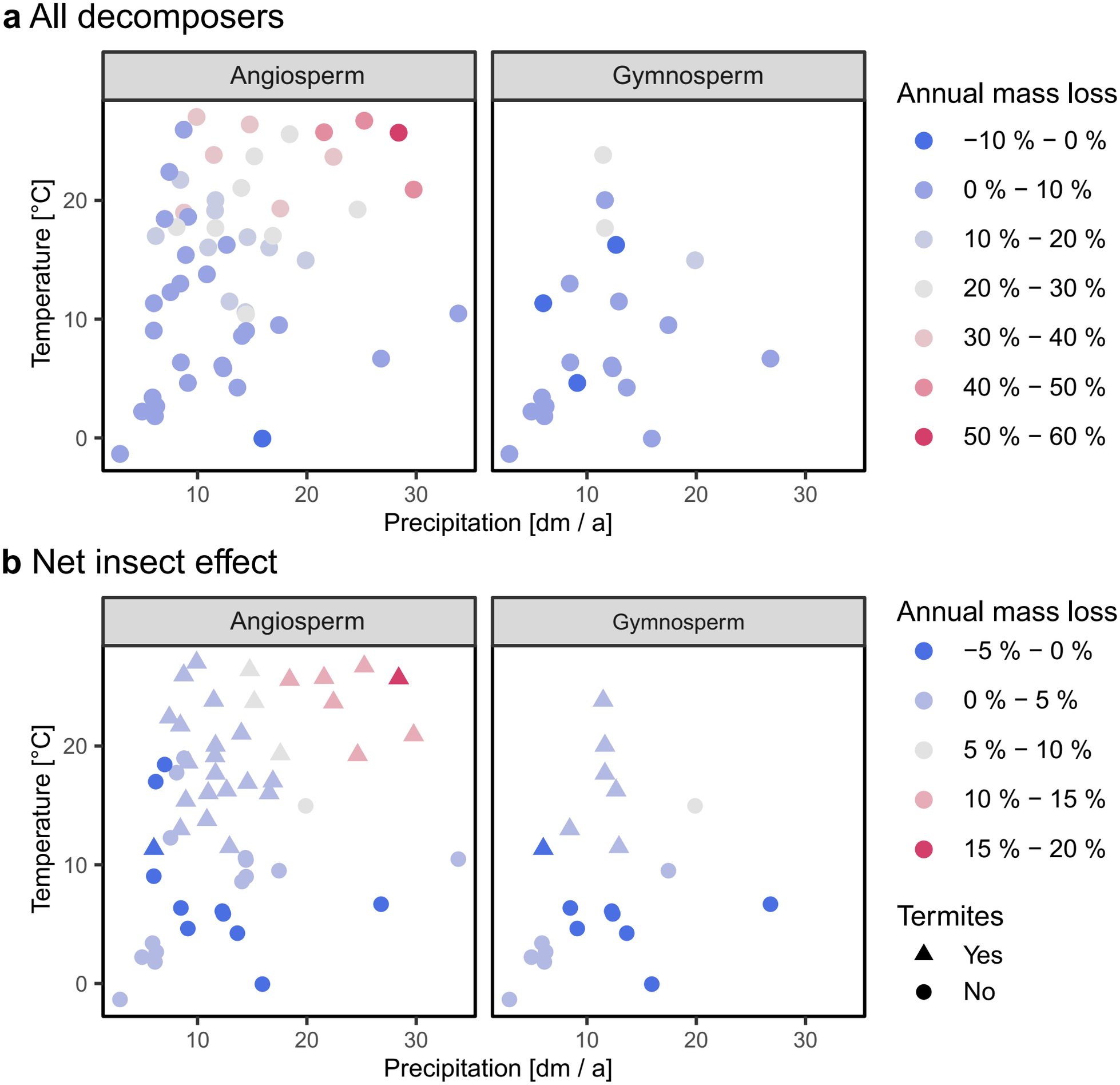
a All decomposers
Angiosperm
Gymnosperm
Temperature [°C]
0
10
20
10
20
30
Precipitation [dm / a]
Annual mass loss
−10 % − 0 %
0 % − 10 %
10 % − 20 %
20 % − 30 %
30 % − 40 %
40 % − 50 %
50 % − 60 %
b Net insect effect
Angiosperm
Gymnosperm
Temperature [°C]
0
10
20
10
20
30
Precipitation [dm / a]
Annual mass loss
−5 % − 0 %
0 % − 5 %
5 % − 10 %
10 % − 15 %
15 % − 20 %
Termites
Yes
No

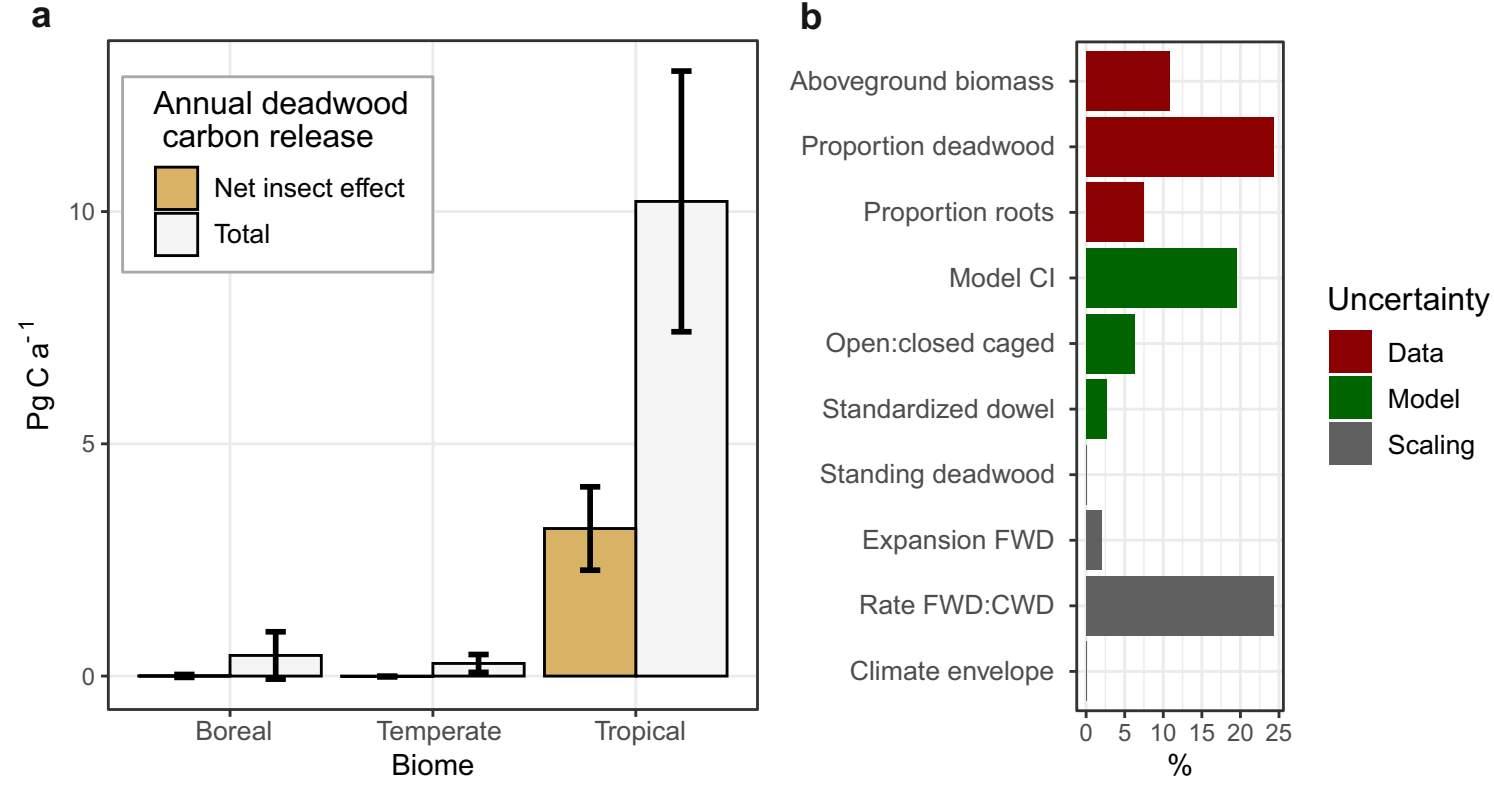
a
Annual deadwood carbon release
Net insect effect
Total
Pg C a-1
10
5
0
Boreal
Temperate
Tropical
Biome
b
Aboveground biomass
Proportion deadwood
Proportion roots
Model CI
Open:closed caged
Standardized dowel
Standing deadwood
Expansion FWD
Rate FWD:CWD
Climate envelope
0 5 10 15 20 25
%
Uncertainty
Data
Model
Scaling

a Arrangement of installations

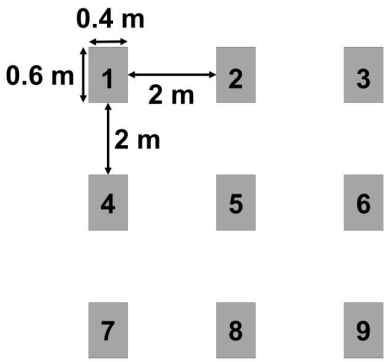

b Closed cage

c Open cage

d Uncaged

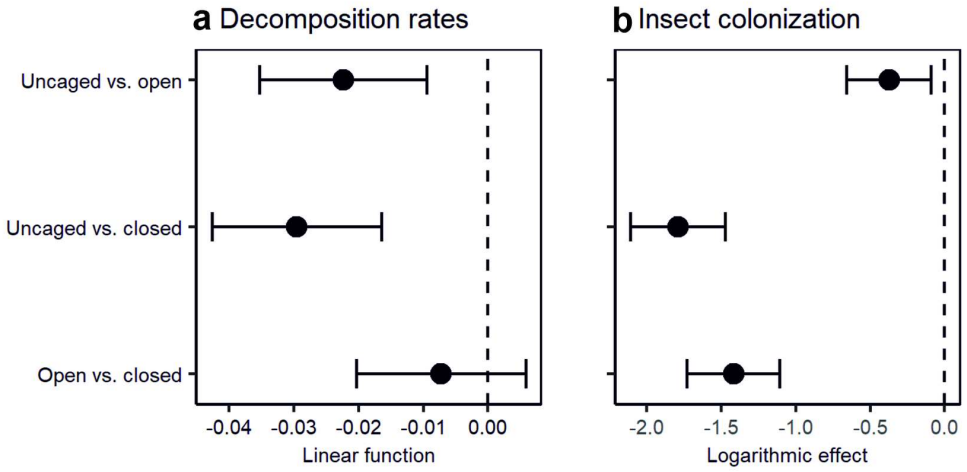
a Decomposition rates
Uncaged vs. open
Uncaged vs. closed
Open vs. closed
-0.04
-0.03
-0.02
-0.01
0.00
Linear function
b Insect colonization
-2.0
-1.5
-1.0
-0.5
0.0
Logarithmic effect

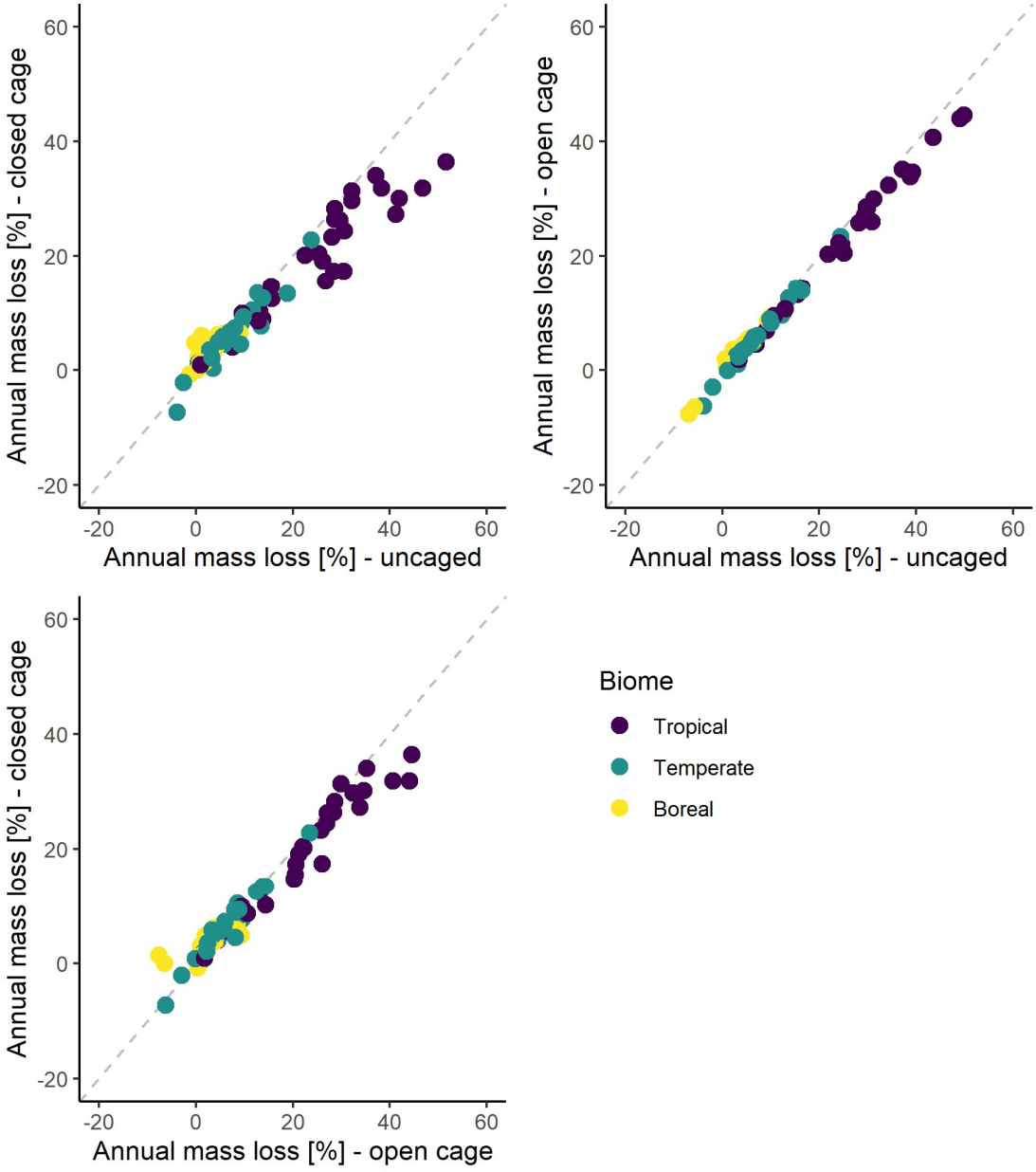
Annual mass loss [%] - closed cage
Annual mass loss [%] - uncaged
Annual mass loss [%] - open cage
Annual mass loss [%] - uncaged
Annual mass loss [%] - closed cage
Annual mass loss [%] - open cage
Biome
Tropical
Temperate
Boreal
60
40
20
0
-20
-20
0
20
40
60

a All decomposers

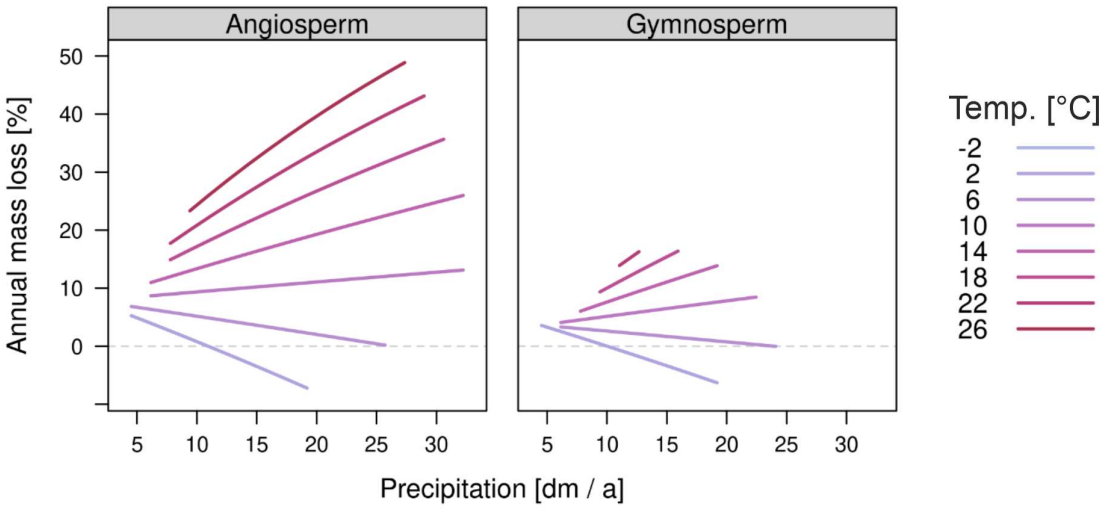

b Net insect effect

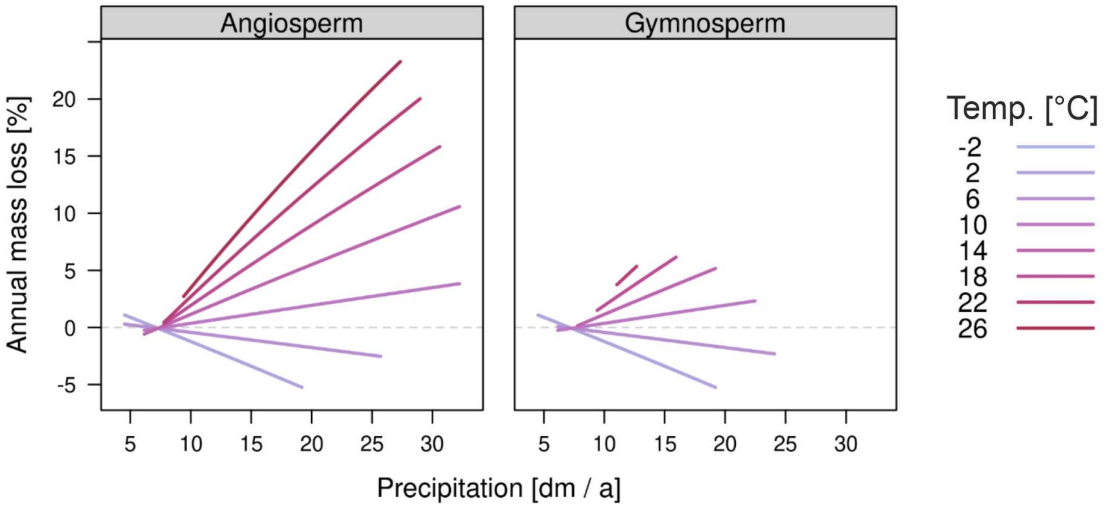

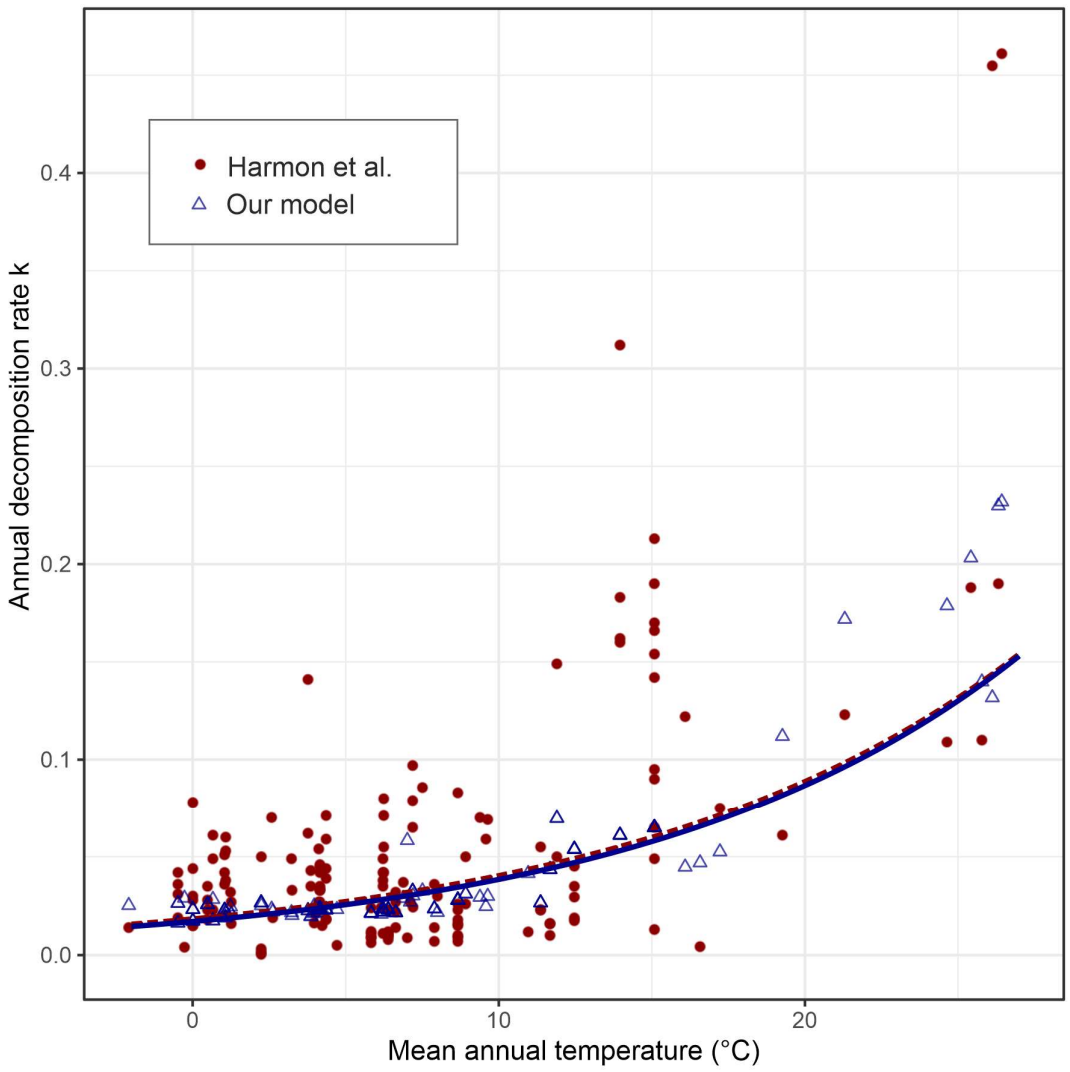
Harmon et al.
Our model
Annual decomposition rate k
0.0
0.1
0.2
0.3
0.4
0
10
20
Mean annual temperature (°C)

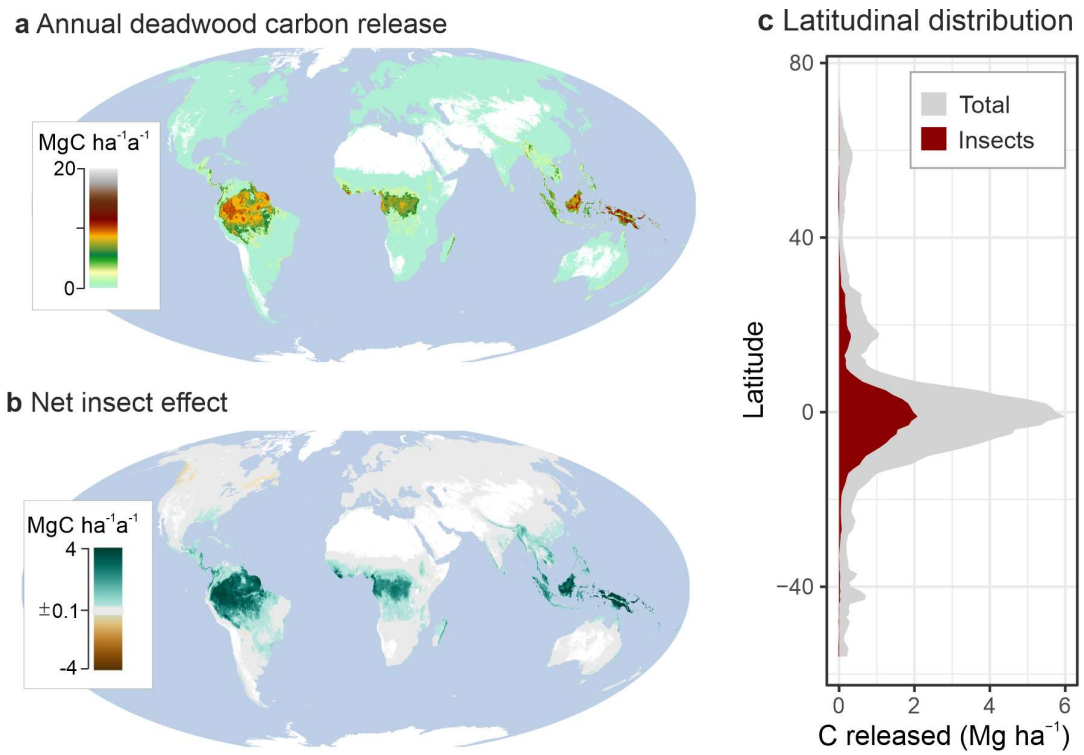
a Annual deadwood carbon release
MgC ha-1a-1
20
0
b Net insect effect
MgC ha-1a-1
4
±0.1
-4
c Latitudinal distribution
80
40
0
−40
Latitude
Total
Insects
0
2
4
6
C released (Mg ha-1)

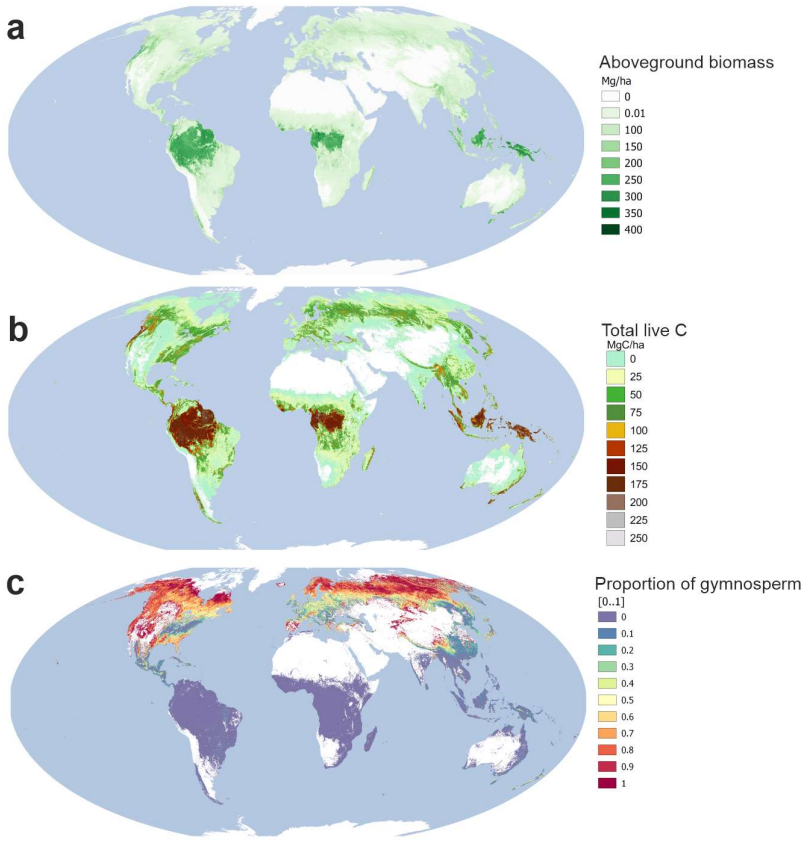
a
Aboveground biomass
Mg/ha
0
0.01
100
150
200
250
300
350
400
b
Total live C
MgC/ha
0
25
50
75
100
125
150
175
200
225
250
c
Proportion of gymnosperm
[0..1]
0
0.1
0.2
0.3
0.4
0.5
0.6
0.7
0.8
0.9
1

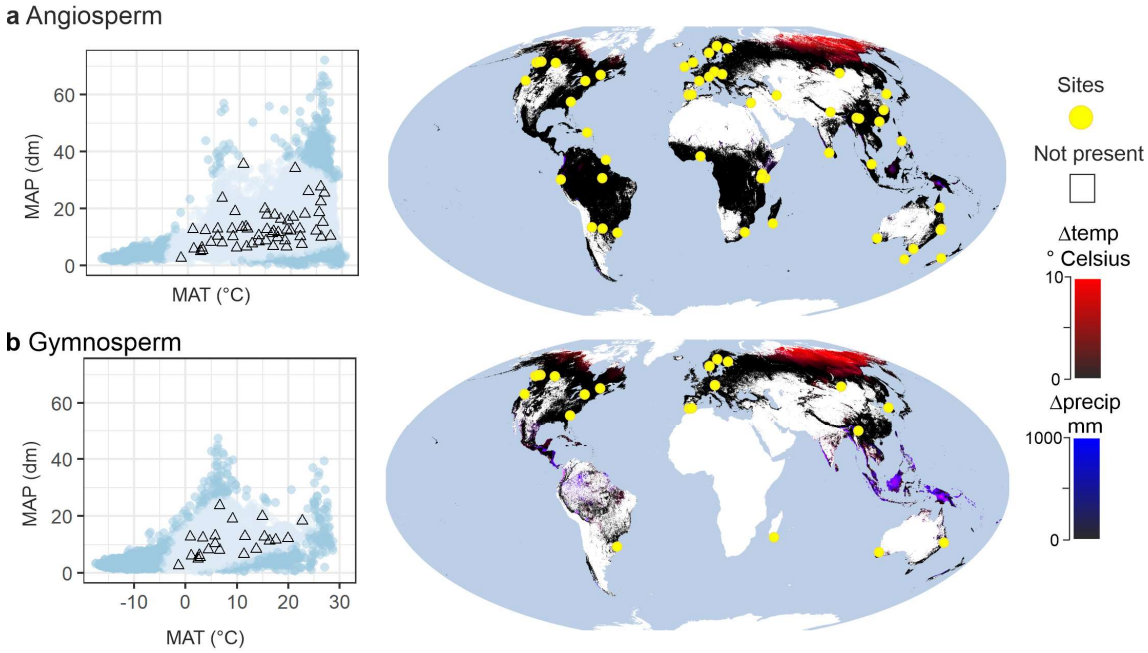
a Angiosperm
MAP (dm)
MAT (°C)
b Gymnosperm
MAP (dm)
MAT (°C)
Sites
Not present
Δtemp
° Celsius
Δprecip
mm